

## ORIGINAL ARTICLE

## Long interspersed element-1 is differentially regulated by food-borne carcinogens via the aryl hydrocarbon receptor

N Okudaira<sup>1,2,8</sup>, T Okamura<sup>3,7</sup>, M Tamura<sup>1</sup>, K Iijima<sup>1</sup>, M Goto<sup>3</sup>, A Matsunaga<sup>1</sup>, M Ochiai<sup>4</sup>, H Nakagama<sup>4</sup>, S Kano<sup>2,5</sup>, Y Fujii-Kuriyama<sup>6</sup> and Y Ishizaka<sup>1</sup>

A single human cell contains more than  $5.0 \times 10^5$  copies of long interspersed element-1 (L1), 80–100 of which are competent for retrotransposition (L1-RTP). Recent observations have revealed the presence of *de novo* L1 insertions in various tumors, but little is known about its mechanism. Here, we found that 2-amino-1-methyl-6-phenylimidazo[4,5-*b*]pyridine (PhIP) and 2-amino-3,8-dimethyl-imidazo[4,5-*f*]quinoxaline (MeIQx), food-borne carcinogens that are present in broiled meats, induced L1-RTP. This induction was dependent on a cellular cascade comprising the aryl hydrocarbon receptor (AhR), a mitogen-activated protein kinase, and CCAAT/enhancer-binding protein  $\beta$ . Notably, these compounds exhibited differential induction of L1-RTP. MeIQx-induced L1-RTP was dependent on AhR nuclear translocator 1 (ARNT1), a counterpart of AhR required for gene expression in response to environmental pollutants. By contrast, PhIP-induced L1-RTP did not require ARNT1 but was dependent on estrogen receptor  $\alpha$  (ER $\alpha$ ) and AhR repressor. *In vivo* studies using transgenic mice harboring the human L1 gene indicated that PhIP-induced L1-RTP was reproducibly detected in the mammary gland, which is a target organ of PhIP-induced carcinoma. Moreover, picomolar levels of each compound induced L1-RTP, which is comparable to the PhIP concentration detected in human breast milk. Data suggest that somatic cells possess machineries that induce L1-RTP in response to the carcinogenic compounds. Together with data showing that micromolar levels of heterocyclic amines (HCAs) were non-genotoxic, our observations indicate that L1-RTP by environmental compounds is a novel type of genomic instability, further suggesting that analysis of L1-RTP by HCAs is a novel approach to clarification of modes of carcinogenesis.

Oncogene (2013) 32, 4903–4912; doi:10.1038/onc.2012.516; published online 3 December 2012

**Keywords:** PhIP; MeIQx; aryl hydrocarbon receptor; breast carcinomas; ER $\alpha$

## INTRODUCTION

Long interspersed element-1 (L1) is the most abundant transposable element, comprising approximately 17% of the human genome.<sup>1</sup> A single cell contains more than  $5.0 \times 10^5$  copies of L1, 80–100 copies of which are competent for retrotransposition (L1-RTP).<sup>1,2</sup> Although approximately 10% of these RTP-competent L1s are highly active, actual occurrence of L1-RTP in the germline has been estimated to be one out of every 108 births.<sup>2,3</sup> L1 encodes two proteins: open reading frames 1 and 2 (ORF1 and 2).<sup>3,4</sup> ORF1 is a 40-kDa protein present within cytoplasmic ribonucleoprotein complexes or stress granules in cytoplasm.<sup>5,6</sup> It acts on L1 mRNA *in cis*<sup>7</sup> and functions as a chaperone of L1 mRNA.<sup>8</sup> By contrast, ORF2 is an approximately 150-kDa protein with both reverse transcriptase<sup>9</sup> and endonuclease<sup>10</sup> activities. ORF2 recognizes the sequence 5'-TAAAA-3' and induces a nick between the T and A,<sup>11,12</sup> leading to first-strand DNA synthesis by target site-primed reverse transcription.<sup>3,4,13</sup> Notably, ORF1 and 2 complete the entire process of L1-RTP<sup>2–4,13</sup> and are competent for the induction of retrotransposition of non-autonomous retroelements, such as Alu<sup>14,15</sup> and SVA (SINE, variable numbers of tandem repeats and Alu).<sup>16</sup>

Vitullo *et al.*<sup>17</sup> recently reported that the copy numbers of mouse L1 were increased during 2–4-blastomere stages. Moreover, it was demonstrated that L1-RTP suppression by blocking reverse transcriptase activity impaired further cellular division.<sup>18</sup> These findings indicate that L1-RTP is a pivotal molecular event in early embryogenesis. However, L1-RTP in oocytes accidentally causes inborn errors: >90 types of intractable diseases were identified as sporadic cases that were caused by mutagenic insertions of endogenous retroelements.<sup>3,4,19</sup> Although most were due to Alu insertions, a recent review indicated the involvement of L1-RTP in 25 sporadic cases of 11 types of genetic disorder.<sup>20</sup> Given the importance of L1-RTP during early embryogenesis, most studies of L1 have focused on germ cells and stem cells.<sup>21–23</sup> However, recent reports of detection of *de novo* L1 and Alu insertions in brain tissues<sup>24–26</sup> and various cancers<sup>27–30</sup> indicate that the mode of RTP in somatic cells is an emerging issue in terms of their biological effects.<sup>31</sup> Intriguingly, a recent report involving use of a highly advanced genome analysis technology identified 194 *de novo* insertions of endogenous retroelements in 43 tumors.<sup>32</sup> Moreover, all of the somatic insertions of L1 or Alu were detected in cancers with epithelial-cell origin, and 64

<sup>1</sup>Department of Intractable Diseases, National Center for Global Health and Medicine (NCGM), Shinjuku-ku, Tokyo, Japan; <sup>2</sup>Graduate School of Comprehensive Human Sciences, University of Tsukuba, Tsukuba, Japan; <sup>3</sup>Department of Laboratory Animal Medicine, National Center for Global Health and Medicine (NCGM), Shinjuku-ku, Tokyo, Japan; <sup>4</sup>Division of Cancer Development System, National Cancer Center Research Institute, Chuo-ku, Tokyo, Japan; <sup>5</sup>Department of Tropical Medicine and Malaria, National Center for Global Health and Medicine (NCGM), Shinjuku-ku, Tokyo, Japan; <sup>6</sup>Institute of Molecular and Cellular Biosciences, The University of Tokyo, Bunkyo-ku, Tokyo, Japan and <sup>7</sup>Section of Animal Model, Department of Infectious Diseases, Tokyo, Japan. Correspondence: Dr Y Ishizaka, Department of Intractable Diseases, National Center for Global Health and Medicine (NCGM), 1-21-1 Toyama, Shinjuku-ku, Tokyo 162 8655, Japan.

E-mail: zakay@ri.ncgm.go.jp

<sup>8</sup>Current address: Department of Legal Medicine, Hyogo College of Medicine, 1-1 Mukogawa-cho, Nishinomiya, Hyogo 663-8501, Japan.

Received 20 April 2012; revised 14 September 2012; accepted 2 October 2012; published online 3 December 2012

insertions were identified in 62 annotated genes, the functions of which were associated with tumor suppression. These observations suggest active involvement of RTP in carcinogenesis.<sup>32</sup> Although the mechanism underlying RTP induction in epithelial cells remains to be elucidated, it is tempting to speculate that environmental factors are involved in the induction of cancer-related L1-RTP.

Reported inducers of L1-RTP in somatic cells include gamma irradiation,<sup>33</sup> heavy metals<sup>34</sup> and benzo[*a*]pyrene (B[*a*]P)<sup>35</sup>. We recently discovered 6-formylindolo[3,2-*b*]carbazole (FICZ), a tryptophan photoproduct, as a potent inducer of L1-RTP.<sup>36</sup> We also found that L1-RTP was induced during two-stage skin carcinogenesis that was initiated by 7,12-dimethylbenzo[*a*]anthracene (DMBA) and 12-*O*-tetradecanoylphorbol-13-acetate.<sup>37</sup> Interestingly, DMBA induction of L1-RTP was dependent on the aryl hydrocarbon receptor (AhR) and AhR nuclear translocator 1 (ARNT1).<sup>38</sup> AhR and ARNT1 are members of the basic helix-loop-helix/pas-arnt-sim (bHLH/PAS) family, which is well conserved among species<sup>39</sup> and comprises transcription factors involved in various biological functions.<sup>40,41</sup> The most well-characterized function of AhR is its binding to environmental pollutants, such as 2,3,7,8-tetrachlorodibenzo-*p*-dioxin, and formation of a complex with ARNT1 (AHR complex), which is recruited to chromatin.<sup>40,41</sup> Notably, chromatin recruitment of the AHR complex depends on the ARNT1 nuclear localization signal.<sup>42</sup>

Here, we report that 2-amino-1-methyl-6-phenylimidazo[4,5-*b*]pyridine (PhIP) and 2-amino-3,8-dimethylimidazo[4,5-*f*]quinoxaline (MeIQx), heterocyclic amines (HCAs) formed during the cooking of red meat,<sup>43,44</sup> induced L1-RTP. Among HCAs, PhIP and MeIQx are important because their levels are high in food.<sup>45</sup> Notably, picomolar levels of PhIP were identified in human breast milk,<sup>46</sup> and HCAs have been shown to be carcinogenic in rodent models.<sup>47–51</sup> PhIP induces carcinoma formation in colon and reproductive organs such as mammary gland and prostate,<sup>47–49</sup> whereas MeIQx induces colon carcinoma and hepatoma.<sup>50,51</sup> These observations imply that humans are exposed daily to carcinogenic compounds, albeit at low concentrations.<sup>52</sup> Here, we present data showing that L1-RTP by both compounds depends on AhR, a mitogen-activated protein kinase (MAPK), and CCAAT/enhancer-binding protein  $\beta$  (C/EBP- $\beta$ ). Interestingly, however, ARNT1 is required for MeIQx-induced L1-RTP but not PhIP-induced L1-RTP. Instead, PhIP-induced L1-RTP depends on estrogen receptor  $\alpha$  (ER $\alpha$ ) and AhRr, a repressor of AhR, another member of the bHLH/PAS family.<sup>53</sup> We also investigated the effects of these HCAs in transgenic mice that harbored human L1 as the transgene.<sup>37</sup> Notably, L1-RTP in the mammary gland was selectively induced by PhIP in an ER $\alpha$ -dependent manner. Taken together with the fact that these compounds did not induce a cellular response that is triggered by DNA damage, we discuss that L1-RTP is a novel mode of carcinogenesis that is induced by non-genotoxic effects of environmental carcinogens.

## RESULTS

We first evaluated HCA-induced L1-RTP using a colony-formation assay, in which L1-RTP induced expression of a functional neomycin-resistant gene, and supported growth of cells cultured in the presence of neomycin. According to the experimental procedures shown in Figures 1a and b, HuH-7 human hepatoma cells were first transfected with pCEP4/L1mneol/ColE1 (pL1-Neo<sup>R</sup>, Figure 1a),<sup>54,55</sup> selected with hygromycin, and then treated with PhIP or MeIQx on day 3 after transfection. Approximately  $5.0 \times 10^5$  cells were treated initially with  $\sim 7.5 \mu\text{M}$  of the synthesized acetoxy-forms of HCAs, which are activated forms of each compound<sup>43,56</sup> (each formula is depicted in Supplementary Figure S1). After neomycin selection, we observed 10–20 colonies on each plate (Figure 1c), indicating that the frequency of L1-RTP induction by both compounds was approximately 1 per  $10^4$

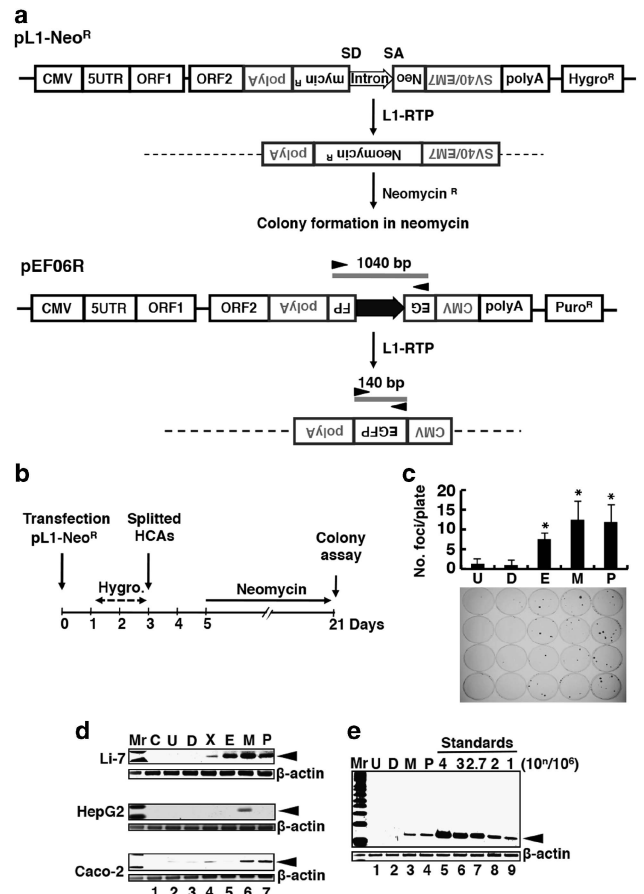


**Figure 1.** HCAs induced L1-RTP. **(a)** Schematics showing the constructs for detecting L1-RTP and the rationale of L1-RTP assay. Upper panel: L1-RTP eliminated an intron, which was placed in exons of neomycin-resistant gene (neomycin<sup>R</sup>), generated a functional neomycin<sup>R</sup> gene and permitted cell growth in the presence of neomycin. Lower panel: The PCR-based assay detected a 140-bp amplified band when L1-RTP was induced. By contrast, a 1040-bp band was amplified without L1-RTP. Arrowheads indicate the positions of primers used for the PCR-based assay. Dotted lines indicate similar structures that correspond to parts of the original L1 reporter constructs. Waved lines indicate genomic DNA. **(b)** Schematic protocols of the colony-formation assay. HuH-7 cells were transfected with pL1-Neo<sup>R</sup>, selected with 25  $\mu\text{g}/\text{ml}$  of hygromycin (Hygro.) and exposed to HCAs. Cells were then cultured in the presence of 800  $\mu\text{g}/\text{ml}$  of neomycin, and numbers of colony were counted on day 21. **(c)** Results of colony-formation assay. U, untreated; D, 0.05% DMSO; M, 35  $\mu\text{M}$  of MeIQx; P, 35  $\mu\text{M}$  of PhIP; E, 35  $\mu\text{M}$  ethylnitrosourea. After selection with neomycin, the cells were stained with methylene blue (low panel) and the number of colonies in five plates in each sample was counted (upper panel). Cell viability after exposure to each compound exceeded 90%. The mean numbers  $\pm$  s.d. are shown. \**P* < 0.01. **(d)** HCA-induced L1-RTP in various human cell lines. For the PCR-based assay, cells were transfected with pEF06R, selected for 2 days with 0.5  $\mu\text{g}/\text{ml}$  of puromycin and then exposed to HCAs. On day 2 after treatment of HCAs, genomic DNA was subjected to the PCR-based assay. Lane 1, cells without pEF06R (C); lane 2, untreated cells with pEF06R (U); lane 3, DMSO (D); lane 4, 4.5 Gy X-ray (X); lane 5, ethylnitrosourea at 70  $\mu\text{M}$  (E); lane 6, MeIQx at 70  $\mu\text{M}$  (M); lane 7, PhIP at 70  $\mu\text{M}$  (P). Arrowhead indicates the PCR product that was generated by L1-RTP. **(e)** L1-RTP was induced by picomolar HCAs. The signal intensities of the amplified PCR products were compared with those derived from standard samples that contained  $1-10^4$  EGFP-positive cells mixed in  $10^6$  control cells (lanes 5–9).<sup>36</sup> Lane 1, untreated (U); lane 2, DMSO (D); lane 3, MeIQx at 3.5  $\mu\text{M}$  (M); lane 4, PhIP at 3.5  $\mu\text{M}$  (P). Arrowhead indicates the PCR product that was generated by L1-RTP. CMV, cytomegalovirus; Mr, molecular weight marker; SD, splicing donor; SA, splicing acceptor; UTR, untranslated region.

(\* $P < 0.01$ ). The induction of L1-RTP by each compound was also evaluated using a PCR-based assay that involved detection of a 140-bp band amplified from a functional *EGFP* (enhanced green fluorescent protein) cDNA in pEF06R, a reporter construct (Figure 1a).<sup>33</sup> As shown in Figure 1d, both compounds induced L1-RTP in different cell lines, including Li-7 (human hepatoma), HepG2 (human hepatoma) and Caco-2 (colon carcinoma). We then determined whether low doses of HCAs induced L1-RTP. As shown in Figure 1e, even 3.5  $\mu\text{M}$  of PhIP and MelQx induced L1-RTP in HuH-7 cells, at a frequency of approximately 1 per  $10^5$  (Figure 1e, lanes 3 and 4) when judged by the signal densities of the 140-bp band normalized by  $\beta$ -actin. Importantly, no cytotoxic effects of the compounds at concentration up to 46  $\mu\text{M}$  were detected (Figure 2a). Moreover, both compounds at 17.5 or 8.8  $\mu\text{M}$ , respectively, did not induce expression of  $\gamma$ -H2AX (Figure 2b), and we detected no focus formation of  $\gamma$ -H2AX or phosphorylated ATM (ataxia telangiectasia mutated) upon treatment of cells with the compounds at 23  $\mu\text{M}$  (Figure 2c). Taken together, these observations indicate that induction of L1-RTP by micromolar HCA levels was attributable to the non-genotoxic effects of the compounds.

To determine the mode of HCA-induced L1-RTP, we first investigated the involvement of AhR, a cellular binding molecule for these compounds.<sup>57</sup> Initially, we tested the effects of 3'-methoxy-4'-nitroflavone (MNF), an AhR inhibitor,<sup>36,37,58</sup> this compound completely blocked L1-RTP induction (Supplementary Figure S2, lanes 7 and 8). To further demonstrate this AhR dependency, we examined the effects of small interfering RNA (siRNA) on *AhR*. First, we confirmed that both of two different *AhR*

siRNAs reduced the expression of endogenous protein (Figure 3a, lanes 4 and 5). The PCR-based assay was then carried out after *AhR* siRNA transfection. As shown in Figure 3b, the induction of L1-RTP by both HCAs was blocked by one of the *AhR* siRNAs (ⓐ in Figure 3a). The other *AhR* siRNA (ⓑ in Figure 3a) also attenuated L1-RTP (Supplementary Figure S3).

We next studied the necessity of ARNT1 for L1-RTP induction using *ARNT1* siRNAs that efficiently reduced the expression of endogenous protein (a representative result of the two siRNAs is shown in Figure 3c and Supplementary Figure S4a; see also Supplementary Figure S3a for results of another *ARNT1* siRNA). Similar to *AhR* siRNA, *ARNT1* siRNA markedly reduced MelQx-induced L1-RTP (Figure 3d, lane 11). Interestingly, however, it did not reduce PhIP-induced L1-RTP (Figure 3d, lane 12). As reported previously, we confirmed that the *AhR* and *ARNT1* siRNAs abolished the expression of *CYP1A1*, a target gene expressed in response to FICZ,<sup>59</sup> indicating that each siRNA effectively abolished the endogenous function of the AHR complex. We also investigated the involvement of AhRR in HCA-induced L1-RTP. By western blot (WB) analysis using an antibody to AhRR ( $\alpha$ AhRR) (Figure 3e)<sup>60</sup> we confirmed that two different *AhRR* siRNAs efficiently down-regulated endogenous AhRR protein. Then, we discovered that transfection of *AhRR* siRNA attenuated L1-RTP induction by PhIP. By striking contrast, it did not affect L1-RTP by MelQx. Taken together, these data suggest that PhIP and MelQx induced L1-RTP via different mechanisms.

Picomolar quantity of PhIP exerts growth-promoting effects that are ER $\alpha$ -dependent.<sup>52</sup> To show the involvement of ER $\alpha$  in PhIP-induced L1-RTP, we determined the effects of fulvestrant, an ER $\alpha$

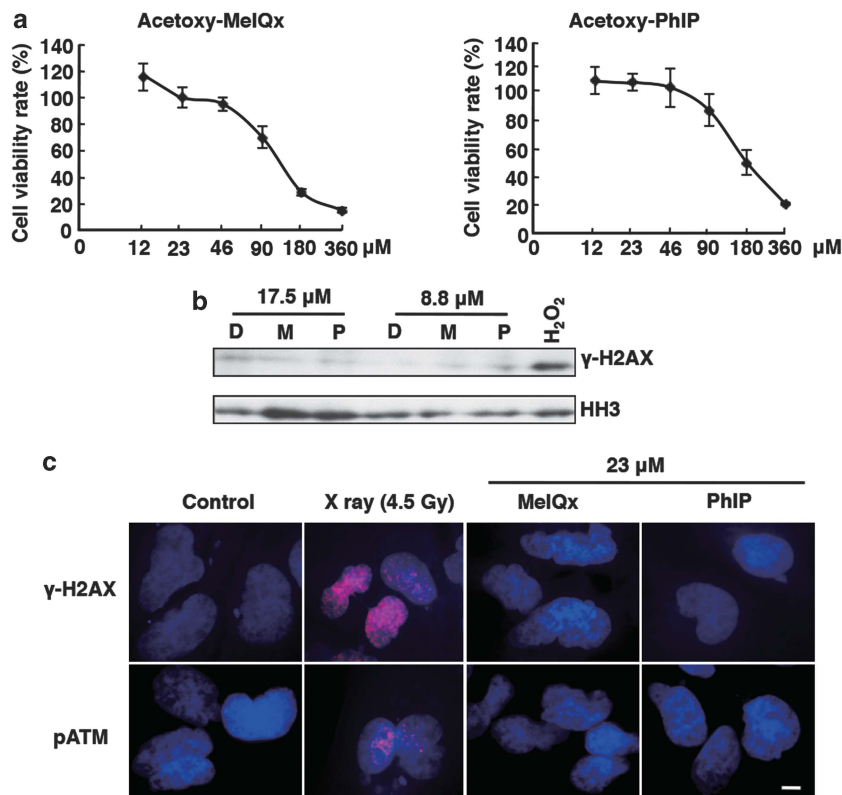


**Figure 2.** No genotoxic activity of HCAs at doses competent for the induction of L1-RTP. **(a)** No cytotoxicity by 12–46  $\mu\text{M}$  levels of HCAs. Approximately  $5 \times 10^5$  cells were treated for 2 days with various doses of HCAs, and the number of colonies was counted after 2 weeks and compared. Effects of each dose were assayed in triplicates. **(b)** No induction of DNA damages. WB analysis was done on cells that had been treated for 2 days with 8.8 or 17.5  $\mu\text{M}$  of HCAs. Samples treated with DMSO (D) at the same concentration as the dose of MelQx (M) or PhIP (P) were also included.  $\text{H}_2\text{O}_2$  (1 mM) is positive control. HH3 is histone H3 as a loading control. **(c)** Immunohistochemical analysis for detecting cellular markers of DNA damage. After treating HuH-7 cells for 2 days with 23  $\mu\text{M}$  of HCAs, the expression of  $\gamma$ -H2AX and ATM phosphorylated at serine 1981 (pATM) was examined. Bar = 10  $\mu\text{m}$ .

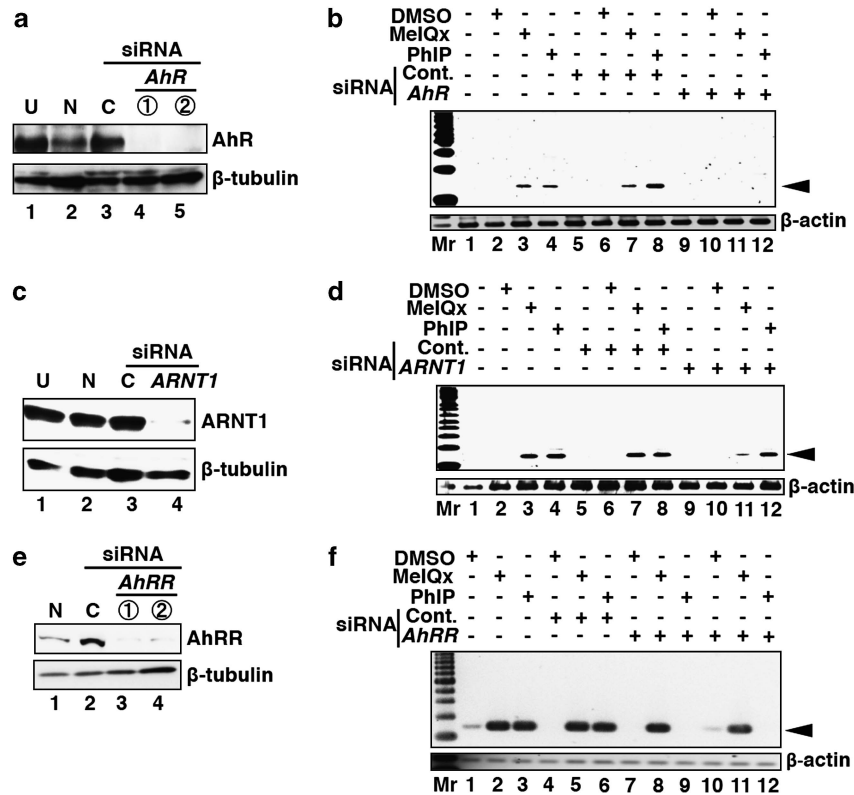


**Figure 3.** HCA-induced L1-RTP depended on AhR. HuH-7 cells were transfected with pEF06R and subjected to the PCR-based assay. **(a)** Knock down of endogenous AhR by siRNA. Effects of two different *Ahr* siRNAs on the expression of endogenous AhR protein were examined in HuH-7 cells with pEF06R (lanes 4 and 5). Lane 1, untreated (U); lane 2, control cells without siRNA (N); lane 3, control siRNA (C); lanes 4 and 5, two different *Ahr* siRNAs (*Ahr*). **(b)** Effects of *Ahr* siRNA on the HCA-induced L1-RTP. One representative result of independent two experiments performed with two different siRNAs was shown. HCA-induced L1-RTP was examined with control siRNA (lanes 5–8) or *Ahr* siRNA (lanes 9–12). HuH-7 cells were treated with 35  $\mu$ M PhIP and MelQx. See also Supplementary Figure S3a for results obtained by another siRNA. **(c)** Down-regulation of endogenous ARNT1 by siRNA. Effects of *ARNT1* siRNA on the expression of endogenous protein were examined in HuH-7 cells with pEF06R (lane 4). Lane 1, untreated (U); lane 2, control cells without siRNA (N); lane 3, control siRNA (C); lane 4, *ARNT1* siRNA (*ARNT1*). One representative result of independent two experiments performed with two different siRNAs was shown (see also Supplementary Figure S4a). **(d)** Effects of *ARNT1* siRNA on HCA-induced L1-RTP. Results of HCA-induced L1-RTP with control siRNA (lanes 5–8) or *ARNT1* siRNA (lanes 9–12) are shown. Lanes 1–4, no siRNAs. See also Supplementary Figure S3a for results obtained by another siRNA. **(e)** Down-regulation of endogenous AhRR by siRNA. Effects of two different *AhRR* siRNAs on the expression of endogenous AhRR protein were examined in HuH-7 cells with pEF06R (lanes 3 and 4). Lane 1, control cells without siRNA (N); lane 2, control siRNA (C); lanes 3 and 4, two different *AhRR* siRNAs (*AhRR*). **(f)** Effects of *AhRR* siRNA on the HCA-induced L1-RTP. HCA-induced L1-RTP was examined with control siRNA (lanes 4–6) or *AhRR* siRNA (lanes 7–12). HuH-7 cells were treated with 35  $\mu$ M PhIP and MelQx. Mr, molecular weight marker.

inhibitor.<sup>61</sup> Consistent with the previous report,<sup>61</sup> the addition of fulvestrant to the culture of MCF-7 human breast carcinoma cells down-regulated ER $\alpha$  expression (Figure 4a). Next, we investigated the effects of fulvestrant on the induction of L1-RTP by PhIP. Notably, fulvestrant selectively attenuated PhIP-induced L1-RTP (Figure 4b, compare lanes 3 and 7), whereas it did not attenuate MelQx-induced L1-RTP (Figure 4b, lanes 2 and 6). We also observed that ER $\alpha$  siRNA completely blocked PhIP-induced L1-RTP (a representative result of the two siRNAs is shown in Figures 4c and d, lanes 11 and Supplementary Figures S3b and 4b). By striking contrast, MelQx-induced L1-RTP was resistant to ER $\alpha$  siRNA. Interestingly, a non-acetoxy form of PhIP, which is present in the human diet as a major subclass,<sup>44,45</sup> also induced L1-RTP (Figure 4b, lane 4; Figure 4d, lane 4). Notably, L1-RTP was again blocked by inhibition of ER $\alpha$  (Figure 4b, lane 8; Figure 4d, lanes 8 and 12).

Based on an observation that ligand-bound AhR activates MAPKs,<sup>62</sup> we next examined the involvement of MAPKs in HCA-induced L1-RTP. Consistent with our previous observations,<sup>36,37,63</sup> L1-RTP was effectively blocked by SB202190 and SP600125, inhibitors of p38 and JNK (Janus kinase), respectively. The

PCR-based assay also revealed the inhibitory effects of both compounds on L1-RTP (Supplementary Figure S5). Interestingly, WB analysis showed that the compounds markedly phosphorylated C/EBP- $\beta$ , a substrate of p38 (Figure 5b, lanes 3 and 4). Moreover, *Ahr* siRNA abrogated HCA-induced phosphorylation of C/EBP- $\beta$  (Figure 5c, lanes 7 and 8), and the down-regulation of C/EBP- $\beta$  siRNA attenuated HCA-induced L1-RTP (Figure 5d, lanes 11 and 12 and Supplementary Figures S3c and 4c). These data strongly suggest that both AhR-dependent activation of MAPKs and C/EBP- $\beta$  phosphorylation are involved in HCA-induced L1-RTP.

ORF1 is localized in cytoplasmic ribonucleoprotein complexes or cytoplasmic stress granules,<sup>5,6</sup> which prompted us to determine whether ORF1 is recruited to chromatin upon exposure of cells to HCAs. To demonstrate this, we performed a subcellular fractionation analysis of ORF1 after transfection of expression vectors encoding a chimeric ORF1-TAP protein.<sup>64</sup> When the transfectants were treated with MelQx or PhIP, the amount of ORF1 in the chromatin-rich fraction was increased without apparent changes in the total amount of ORF1 (Figure 6a, lanes 2 and 3). Notably, ORF1 was detected only when the nuclear-insoluble fractions were treated with micrococcal nuclease

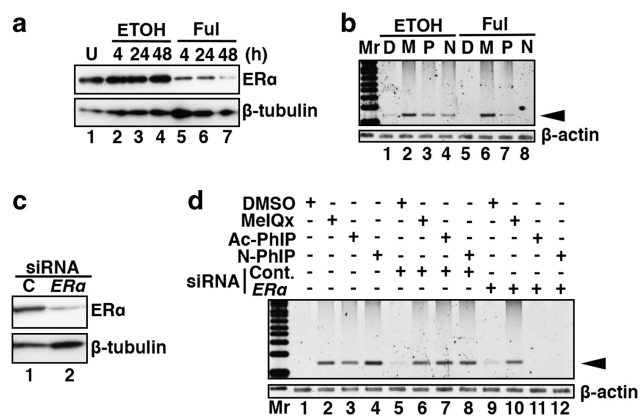


**Figure 4.** PhIP-induced L1-RTP depended on ER $\alpha$ . **(a)** Effects of an ER $\alpha$  inhibitor on the expression of ER $\alpha$ . Fulvestrant, an inhibitor of ER $\alpha$ , was treated at 100 nM for 4, 24 and 48 h. Then, cell extracts were prepared and subjected to WB analysis. U, untreated; ETOH, ethanol; Ful, fulvestrant. **(b)** PhIP-induced L1-RTP depended on ER $\alpha$ . Effects of fulvestrant added 4 h before the addition of HCAs were shown. Lanes 1–4, ethanol (ETOH); lane 5–8, fulvestrant at 100 nM (Ful). Lanes 1 and 5, DMSO (D); lanes 2 and 6, MelQx (M); lanes 3 and 7, acetoxy-form PhIP (P); lanes 4 and 8, non-acetoxy form PhIP (N). **(c)** Effects of ER $\alpha$  siRNA on the expression of endogenous protein. Expression of endogenous ER $\alpha$  protein was examined in MCF-7 cells that had been transfected with pEF06R and ER $\alpha$  siRNA. Lane 1, control siRNA (C); lane 2, ER $\alpha$  siRNA (ER $\alpha$ ). **(d)** Inhibition of PhIP-induced L1-RTP by ER $\alpha$  siRNA. One representative result of independent two experiments performed with two different siRNAs was shown (see also Supplementary Figures S3b and 4b). Lanes 1–4, no siRNAs; lanes 5–8, control siRNA (Cont.); lanes 9–12, ER $\alpha$  siRNA. Mr, molecular weight marker.

(Figure 6b, lanes 11 and 12). Notably, HCA-induced chromatin recruitment of ORF1 was blocked by both *Ahr* siRNA (a representative result of the two siRNAs is shown in Figure 6c, lanes 5 and 6 and Supplementary Figure S6a) and MAPK inhibitors (Figure 6d, lanes 5, 6, 8 and 9). Moreover, the PhIP-induced chromatin recruitment of ORF1 was blocked by *AhrR* siRNA (a representative result of the two siRNAs is shown in Figure 6e, lanes 6 and Supplementary Figure S6b) and fulvestrant (Figure 6f, lane 6).

The chromatin recruitment of ORF1 suggests its association with ER $\alpha$ . To investigate this possibility, we transfected MCF-7 cells with pORF1-EGFP encoding a chimeric ORF1-EGFP protein, treated them with HCAs and performed immunoprecipitation (IP) followed by WB analysis. IP with  $\alpha$ ER $\alpha$  followed by WB analysis with  $\alpha$ EGFP definitely revealed that ORF1 associated with ER $\alpha$  upon PhIP treatment (Figure 7a, lane 6, arrow). However, this was not the case for MelQx (lane 5). Moreover, a reciprocal experiment, in which IP was performed using  $\alpha$ EGFP followed by WB analysis using  $\alpha$ ER $\alpha$ , detected the interaction of ORF1 and ER $\alpha$  in PhIP-treated cells (Figure 7b, lane 6, arrow). We next determined whether ORF1 formed a complex with C/EBP- $\beta$ . IP-WB analysis using expression vectors encoding streptag-ORF1 (pST-ORF1) and flag-tagged C/EBP- $\beta$  (pFlag-C/EBP- $\beta$ ) revealed that these two molecules were constitutively associated (Figure 7c, lane 4, Be: bead). By contrast, flag-tagged ovalbumin (OVA) was not associated with ST-ORF1 under the same conditions (lane 2), indicating that the interaction of these molecules was not due to a non-specific binding property of ORF1. Conversely, a reciprocal experiment confirmed the association of C/EBP- $\beta$  and ORF1 (Figure 7d). Taken together, these data indicate that ORF1 constitutively forms a complex with C/EBP- $\beta$  and that it can associate with ER $\alpha$  in response to the addition of PhIP.

To examine whether the HCAs induced L1-RTP *in vivo*, we used hL1-EGFP mice (No. 4 and No. 67).<sup>37</sup> In our previous work, we

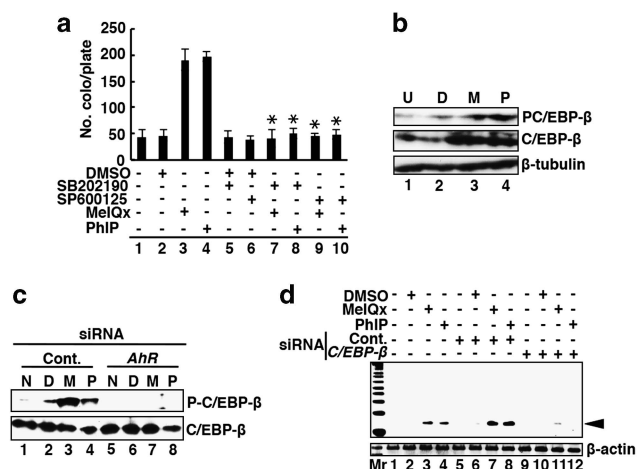


**Figure 5.** HCA-induced L1-RTP required MAPK activity and C/EBP- $\beta$ . **(a)** Effects of MAPK inhibitors on L1-RTP. HuH-7 cells were transfected with pL1-Neo<sup>R</sup>, exposed to 17.5  $\mu$ M HCAs with or without MAPK inhibitors, which were added 0.5 h before the addition of HCAs, and subjected to colony-formation assay. Both SB202190 and SP600125 significantly attenuated L1-RTP by MelQx (lanes 7 and 9) and PhIP (lanes 8 and 10). \* $P$  < 0.01. **(b)** HCAs phosphorylated C/EBP- $\beta$ . HuH-7 cells were treated with micromolar of each HCA. Lane 1, untreated (U); lane 2, DMSO (D); lane 3, MelQx at 17.5  $\mu$ M (M); lane 4, PhIP at 17.5  $\mu$ M (P). **(c)** The phosphorylation of C/EBP- $\beta$  depended on *Ahr*. HCA-induced phosphorylation of C/EBP- $\beta$  was examined in HuH-7 cells that had been transfected with *Ahr* siRNA. Lanes 1 and 5, non-treated (N); lanes 2 and 6, DMSO (D); lanes 3 and 7, 17.5  $\mu$ M MelQx (M); lanes 4 and 8, 17.5  $\mu$ M PhIP (P). **(d)** C/EBP- $\beta$  was required for HCA-induced L1-RTP. Effects of C/EBP- $\beta$  siRNA on HCA-induced L1-RTP in HuH-7 cells were examined. One representative result of independent two experiments performed with two different siRNAs was shown (see also Supplementary Figures S3c and 4c). Lanes 1–4, no siRNA; lanes 5–8, control siRNA (Cont.); lanes 9–12, C/EBP- $\beta$  siRNA.

proved that these mice were suitable for studying the modes of L1-RTP in somatic cells, because these mice possessed low background of L1-RTP during embryogenesis, but they responded for induction of L1-RTP in response to environmental carcinogens.<sup>37</sup> When the mice were injected intraperitoneally with 3 nM of HCAs three times (estimated in blood concentration), L1-RTP was detected in the bone marrow (Figure 8a). Notably, PhIP induced L1-RTP in the mammary gland and colon, whereas MelQx induced L1-RTP in the liver, spleen and gastric mucosa (one representative result of three independent experiments are shown). To determine whether HCA-induced L1-RTP is also dependent on the *Ahr* gene, we used homozygous null *Ahr* (*Ahr*<sup>-/-</sup>) mice.<sup>65</sup> No induction of HCA-induced L1-RTP was observed in No. 4h L1-EGFP/*Ahr*<sup>-/-</sup> mice (Figure 8b, lanes 8 and 9) or in No. 67 hL1-EGFP/*Ahr*<sup>-/-</sup> mice (Supplementary Figure S7). To exclude the possibility that hL1-EGFP/*Ahr*<sup>-/-</sup> mice possessed defective cellular machinery required for the induction of L1-RTP, we examined the induction of L1-RTP by FICZ. Consistent with our previous observation that FICZ-induced L1-RTP was not *Ahr*-dependent<sup>36</sup> the administration of FICZ robustly induced L1-RTP in the thymus, lymph node and liver of hL1-EGFP/*Ahr*<sup>-/-</sup> mice (Supplementary Figure S8). The data indicate that L1-EGFP/*Ahr*<sup>-/-</sup> mice were competent for L1-RTP and HCA-induced L1-RTP was *Ahr*-dependent. Interestingly, L1-RTP was occasionally identified in hL1-EGFP/*Ahr*<sup>+/-</sup> mice (Figure 8b, lane 5). A plausible explanation is that the amount of *Ahr* protein derived from the intact single allele of the *Ahr* gene is sufficient for the induction of L1-RTP.

We further tested whether lower doses of the HCAs resulted in induction of L1-RTP. After 3 pM of the HCAs were injected intraperitoneally three times per week for 6 weeks, mammary

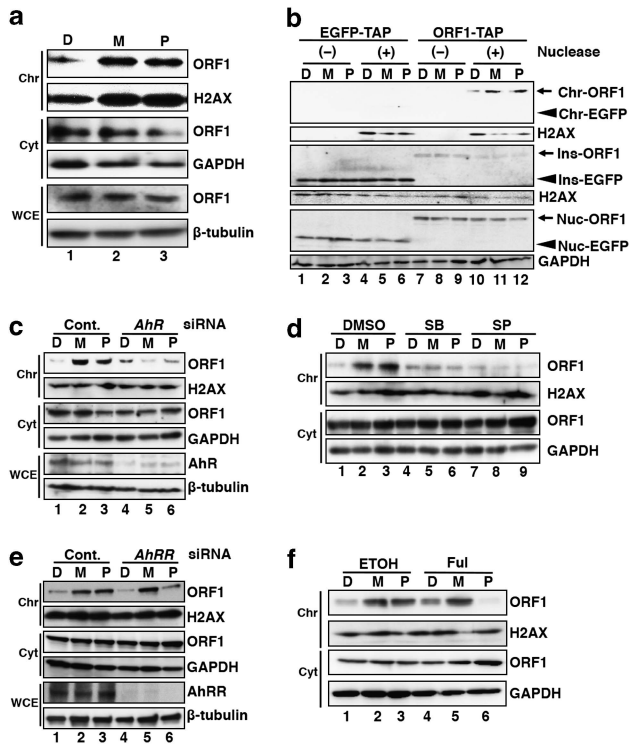


**Figure 6.** HCA-induced chromatin recruitment of ORF1 coupled with the induction of L1-RTP. HuH-7 or MCF-7 cells were transfected with pORF1-TAP<sup>64</sup> and WB analysis was done on fractionated extracts of cells treated with HCAs for 24 h. (a) Recruitment of ORF1 to the chromatin-rich fraction by HCAs. ORF1 in chromatin (Chr) and cytoplasmic (Cyt) fractions, and whole-cell extract (WCE) were examined in HuH-7 cells. Lane 1, DMSO (D); lane 2, MelQx at 17.5  $\mu$ M (M); lane 3, PhIP at 17.5  $\mu$ M (P). (b) ORF1 was present in the chromatin-rich fraction. Nuclear insoluble fractions prepared after treatment with HCAs were treated with micrococcal nuclease, and the supernatant after centrifugation was subjected to WB analysis. Antibodies to H2AX ( $\alpha$ H2AX) and GAPDH ( $\alpha$ GAPDH) were used to show that the analyzed samples contained chromatin components and cytoplasmic fractions, respectively. Both pellet after centrifugation (Ins-ORF1) and aliquots of nuclear fractions (Nuc-ORF1) were analyzed. Cells were transfected with pEGFP-TAP (lanes 1–6), whereas with pORF1-TAP (lanes 7–12). Lanes 1, 4, 7 and 10, DMSO (D); lanes 2, 5, 8 and 11, MelQx at 17.5  $\mu$ M (M); lanes 3, 6, 9 and 12, PhIP at 17.5  $\mu$ M (P). (c) Effects of *AhrR* siRNA on HCA-induced chromatin recruitment of ORF1. HuH-7 cells transfected with pORF1-TAP with control (lanes 1–3) or *AhrR* siRNAs (lanes 4–6). After 2 days cells were treated for 24 h with HCAs, and fractionated cellular extracts were subjected to WB analysis. Lanes 1 and 4, DMSO (D); lanes 2 and 5, MelQx at 17.5  $\mu$ M (M); lanes 3 and 6, PhIP at 17.5  $\mu$ M (P). One representative result of independent two experiments performed with two different siRNAs was shown (see also Supplementary Figure S6a). (d) MAPK inhibitors blocked HCA-induced chromatin recruitment of ORF1. The similar fractionation analysis described in Figure 6c was done. Cells were treated with inhibitors of p38 (SB202190, SB) and JNK (SP600125, SP), which were added 0.5 h before the addition of 17.5  $\mu$ M HCAs. (e) Effects of *AhRR* siRNA on HCA-induced chromatin recruitment of ORF1. By using *AhRR* siRNA, the similar experiment shown in Figure 6c was done. One representative result of independent two experiments performed with two different siRNAs was shown (see also Supplementary Figure S6b). (f) Effects of fulvestrant on HCA-induced chromatin recruitment of ORF1. MCF-7 cells were transfected with pORF1-TAP and treated with 17.5  $\mu$ M HCAs and 100 nM fulvestrant (Ful). Fulvestrant was added 4 h before the addition of HCAs, and cells were harvested after 24 h after the addition of HCAs. WB analysis was done on chromatin (Chr) and cytoplasmic (Cyt) fractions. Lanes 1 and 4, DMSO (D); lanes 2 and 5, MelQx at 17.5  $\mu$ M (M); lanes 3 and 6, PhIP at 17.5  $\mu$ M (P). ETOH, ethanol; GAPDH, glyceraldehyde 3-phosphate dehydrogenase.

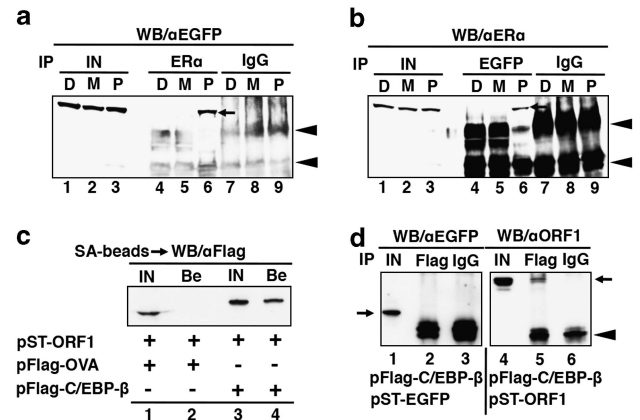


**Figure 7.** PhIP induced association of ORF1 and ER $\alpha$ . (a) ORF1 associated with ER $\alpha$  after treatment with PhIP (P). IP was done with  $\alpha$ ER $\alpha$ , followed by WB with  $\alpha$ EGFP. Arrow indicates a signal of ORF1-EGFP. Arrowhead indicates immunoglobulin G (IgG) heavy chain and IgG light chain. Lanes 1–3, input; lanes 4–6, IP with  $\alpha$ ER $\alpha$ ; lanes 7–9, IP with control IgG. (b) ER $\alpha$  associated with ORF1 after treatment with PhIP. IP was done with  $\alpha$ EGFP, followed by WB analysis with  $\alpha$ ER $\alpha$ . Arrow indicates the signal of ER $\alpha$ . Arrowhead, heavy and light chains of IgG. Lanes 1–3, input; lanes 4–6, IP with  $\alpha$ EGFP; lanes 7–9, IP with control IgG. (c) ORF1 was constitutively associated with C/EBP- $\beta$ . HEK293T cells were transfected with pST-ORF1 and pFlag-OVA (lanes 1 and 2) or pFlag-C/EBP- $\beta$  (lane 3 and 4). Then cell extracts were reacted with dynabeads M-280 streptavidin, and recovered samples were subjected to WB analysis with  $\alpha$ Flag. (d) A reciprocal experiment proved the association of C/EBP- $\beta$  and ORF1. Into HEK293T cells, pFlag-C/EBP- $\beta$  was co-transfected with pST-EGFP (lanes 1–3) or pST-ORF1 (lane 4–6), and cell extracts were immunoprecipitated with  $\alpha$ Flag, followed by WB analysis with  $\alpha$ EGFP or  $\alpha$ ORF1. As control, IgG was used as for IP (lanes 3 and 6). Arrows indicates the position of ST-EGFP (lane 1) or ST-ORF1 (lane 4). Arrow indicates the signal of EGFP (left panel) and ORF1 (right panel). Arrowhead indicates IgG light chain. Be, beads; D, DMSO; IN, input; M, MelQx; PhIP.

gland, colon and liver tissues were subjected to the PCR-based assay. As shown in Figure 8c, PhIP induced L1-RTP in the mammary gland and colon (lanes 9 and 15). Several independent experiments indicated that the repetitive administration of low doses of PhIP reproducibly induced L1-RTP in the mammary gland, whereas MelQx did not (Table 1,  $P < 0.0001$ ). To demonstrate that an orally administered compound is also capable of induction of L1-RTP, we directly injected PhIP into the stomach and evaluated the presence of L1-RTP in the mammary gland. Administration of PhIP of both 6 (Figure 8d, left panel) and 1.8 (Figure 8d, right panel)  $\mu$ M induced L1-RTP in the mammary gland. Finally, we found that the simultaneous injection of fulvestrant abrogated PhIP-induced L1-RTP in the mammary gland (Figure 8e, lane 4).

**DISCUSSION**

Recent advances in genome analysis technology have allowed determination of the numbers of *de novo* L1 insertions in cancers with epithelial-cell origin.<sup>32</sup> Based on information regarding L1 integration sites, a positive role L1-RTP in carcinogenesis has been postulated.<sup>32</sup> Although the mechanism of L1-RTP induction during carcinogenesis remains elusive, our current work supports that environmental carcinogens function as the trigger: both PhIP and MelQx, food-borne carcinogens,<sup>43,44</sup> reproducibly induced L1-RTP *in vitro* and *in vivo*. However, it is important to demonstrate that L1-RTP is induced by HCAs in an endogenous setting because our current observations were obtained by the hL1-EGFP mice, in which multiple copies of human L1 were integrated as the

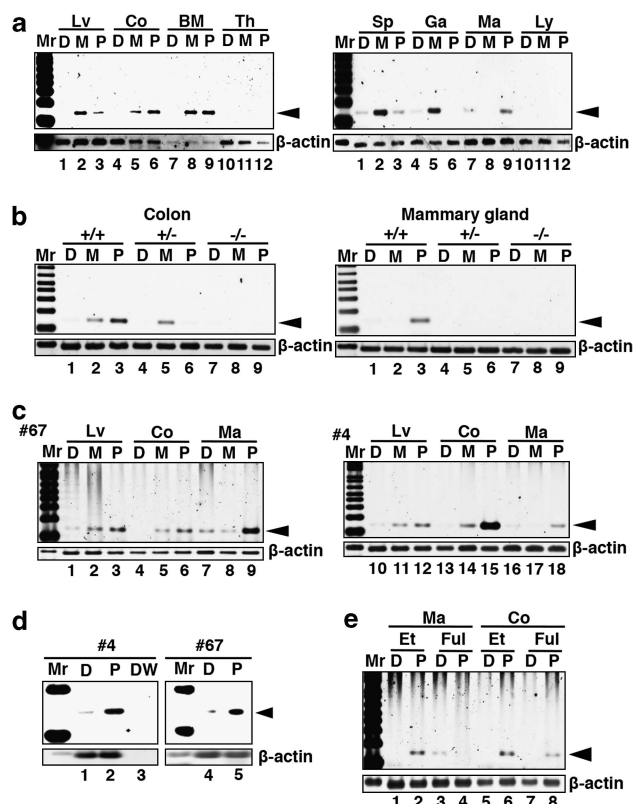


**Figure 8.** HCA-induced L1-RTP in a manner dependent on AhR *in vivo*. L1-RTP was assayed by using L1-EGFP/AhR<sup>-/-</sup> mice. (a) Nanomoles of HCAs induced L1-RTP *in vivo*. Into the hL1-EGFP mice, nanomoles of HCAs were administered three times once every 2 days, and the DNA extracted from the tissues was analyzed. Representative results of No. 4 female L1-transgenic mice are shown. Arrowhead indicates 140 bp derived from the L1 product. (b) HCA-induced L1-RTP was blocked in L1-EGFP/AhR<sup>-/-</sup> mice. HCAs of 3 nM were administered three times once every 2 days, and the DNA extracted from the tissues was analyzed. Representative results of No. 4 hL1-EGFP/AhR<sup>-/-</sup> mice are shown. Results of No. 67 hL1-EGFP/AhR<sup>-/-</sup> mice are demonstrated in Supplementary Figure S7. (c) Repetitive injections of low doses of PhIP selectively induced L1-RTP in the mammary gland. Three pM of HCAs was administered totally 18 times once 2 days at the frequency of three times a week. After 6 weeks, DNA was extracted from each tissue 2 days after the last injection of HCAs. Then extracted DNA was subjected to the PCR-based assay. Results of No. 67 and No. 4 of hL1-EGFP mice are shown. See also Table 1. (d) Orally administered PhIP (P) induced L1-RTP in the mammary gland. In the first experiment, PhIP of 3.3 μg (approximately 12 nanomoles) was directly administered into the stomach of No. 4 hL1-EGFP mouse everyday. After six times of administration, DNA from the mammary gland was subjected to the PCR-based assay. In the second experiment, 1 μg (approximately 3.6 nanomoles) of PhIP was orally administered into No. 67 mouse. After six times of administration, the PCR-based assay was done. If all of the administrated compounds were adsorbed into blood, the volume of which was estimated as approximately 2 ml, the blood concentration of the compound would be 6 μM (first experiments, lane 2) or 1.8 μM (second experiments, lane 5). The same content of DMSO (D), used as a solvent of the compound, was administered (lanes 1 and 4). During the course of experiments, no changes in body weight of mice were observed. Lane 1, DMSO (D); lane 2, PhIP; lane 3, distilled water (DW); lane 4, DMSO; lane 5, PhIP. (e) Fulvestrant (Ful) inhibited PhIP-induced L1-RTP. Fulvestrant of 8 mg/kg was administered 4 h before intraperitoneal injection of 3 pM PhIP. Combined injection of fulvestrant and PhIP was done three times, once every 2 days. Additional injection of fulvestrant was performed 1 day before the administration of PhIP. BM, bone marrow; Co, colon; Ga, gastric mucosa; Lv, liver; Ly, lymph node; Ma, mammary gland; Sp, spleen; Th, thymus. Et, ethanol; D, DMSO; M, MelQx; P, PhIP; Mr, molecular weight marker.

**Table 1.** Summary of L1-RTP induced by HCAs in hL1-EGFP mice

Strains	HCAs	3 nM (× 3)			3 pM (× 18)		
		Ma.	Colon	Liver	Ma.	Colon	Liver
No. 4	PhIP	5/6	6/6	3/6	3/3	3/3	3/3
	MelQx	0/6	4/6	6/6	0/3	3/3	3/3
No. 67	PhIP	3/4	4/4	2/4	3/3	3/3	3/3
	MelQx	0/4	4/4	4/4	0/3	3/3	3/3
Total	PhIP	8/10	10/10	5/10	6/6	6/6	6/6
	MelQx	0/10	8/10	10/10	0/6	6/6	6/6

Abbreviations: EGFP, enhanced green fluorescent protein; HCA, heterocyclic amine; L1-RTP, long interspersed element-1 (L1) competent for retrotransposition; Ma, mammary gland; MelQx, 2-amino-3,8-dimethylimidazo[4,5-f]quinoxaline; PhIP, 2-amino-1-methyl-6-phenylimidazo[4,5-b]pyridine. HCAs were administered into hL1-EGFP mice three times of 3 nM or 18 times of 3 pM, respectively. Representative results are shown in Figure 8. Numbers of samples positive for L1-RTP with relative intensity (RI) more than threefold to control were counted. Total numbers of samples positive for L1-RTP in the mammary gland (Ma.) by two doses of PhIP were 14 (8 + 6) out of 16 (10 + 6) examined, whereas those by MelQx were 0 out of 16 (10 + 6). Difference of the induction of L1-RTP in the mammary gland by PhIP was statistically significant ( $P < 0.0001$ ).

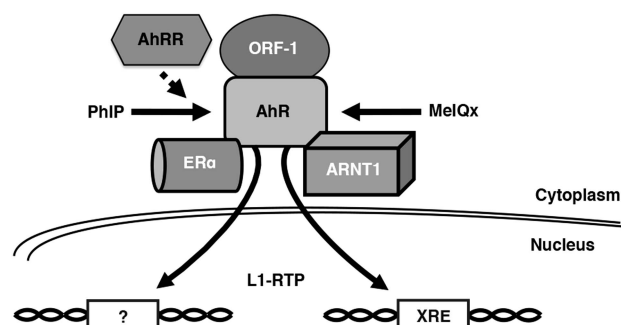


**Figure 9.** Hypothetical modes of L1-RTP differentially regulated by MelQx and PhIP. Based on experimental data, a schematic of L1-RTP by HCAs was described. L1-RTP by MelQx depended on AhR and ARNT1, a classical set of the AHR complex. By contrast, PhIP induces L1-RTP depending on AhR, AhRR and ERα, which might recognize a genome locus different from XRE.

transgene.<sup>37</sup> One approach is to characterize L1-RTP after exposing PhIP to primary cultured human cells that are derived, for example, from mammary gland. By comparison of integration sites of L1 in PhIP-treated cells and *de novo* L1 insertions in breast carcinomas, it might be possible to approach roles of PhIP in carcinogenesis.

Several independent experiments revealed that PhIP selectively induced L1-RTP in the mammary gland. Fourteen out of the 16 PhIP-treated mice examined were positive for L1-RTP in the mammary gland of the hL1-EGFP mice (Table 1). By contrast, no L1-RTP was detected in the corresponding tissue of MelQx-treated mice. Interestingly, biochemical analyses revealed that both compounds induced L1-RTP in an AhR-dependent manner; however, MelQx-induced L1-RTP required ARNT1, whereas PhIP-induced L1-RTP did not require ARNT1 but depended on ERα (Figure 4). The requirement of ERα for PhIP-induced L1-RTP was further supported by data showing that PhIP promoted the association of ORF1 and ERα (Figure 7a). Additionally, the PhIP-induced chromatin recruitment of ORF1 was abrogated by fulvestrant (Figure 6f), implying that the dependency of PhIP-induced L1-RTP on ERα is related to the mode by which PhIP induces malignancies in reproductive organs.<sup>47-49</sup> Also,

PhIP-induced L1-RTP was AhRR-dependent (Figure 3f), and PhIP-induced recruitment of ORF1 to chromatin required AhRR (Figure 6e). AhRR was originally identified as a repressor of AhR,<sup>53</sup> but recent studies suggested AhRR to possess additional activities that include regulatory function in mammalian reproduction.<sup>66</sup> Further analysis may disclose a novel function of AhRR in the responses of cells to environmental carcinogens, such as PhIP.

It has been well-known that ligand-bound AhR associates with ARNT1, forms an AHR complex and is recruited to the XRE, leading to the transcription of genes, such as *CYP1A1*.<sup>39,40</sup> ARNT1 is crucial for this process, because the chromatin recruitment of the AHR complex depends on the nuclear localization signal of ARNT1.<sup>42</sup> As L1-RTP induction by PhIP depended on AhR but not ARNT1, the mode of PhIP-induced L1-RTP is different from the classical cellular cascade of the AHR complex. Moreover, the PhIP-induced chromatin recruitment of ORF1 was dependent on AhR, AhRR and ER $\alpha$  (Figure 6). Data imply that the genomic loci to which ORF1 is recruited in response to PhIP differ from those determined by the AHR complex, and L1 integration sites of PhIP and MeIQx might be different (Figure 9). Further studies are required to investigate this possibility. Although it has been proposed that L1-RTP is regulated at the transcriptional level,<sup>67,68</sup> our analysis using methylation-specific primers<sup>69</sup> detected no changes of the methylation status of the 5' untranslated region of L1 before and after administration of HCAs (Supplementary Figure S9). Additionally, no apparent increase of the expression of L1-mRNA was detected after treatment of HCAs (Supplementary Figure S10). Although it is possible that HCAs transiently modulate the L1 transcript levels, HCA-induction of L1-RTP is likely regulated predominantly at the post-transcriptional level (Supplementary Figure S10).

Notably, we reported previously that environmental carcinogens, such as DMBA, 3-methylcholanthrene and B[a]P induced in an L1-RTP AhR-dependent manner.<sup>63</sup> By contrast, FICZ, a tryptophan photoproduct that is not carcinogenic,<sup>70,71</sup> also exhibited L1-RTP but in an AhR-independent manner. Together with the report that AhR is required for the chemical carcinogenesis caused by B[a]P<sup>72</sup> and that L1-RTP induces a variety of genetic alternations such as gene deletion and chromosomal translocations,<sup>54,73</sup> it is plausible that the AhR-dependent L1-RTP has a positive link with carcinogenesis. Moreover, L1-encoded proteins can induce RTP of other retroelements such as Alu and SVA,<sup>14–16</sup> and non-allelic homologous recombination between *Alu* sequences is known to ablate various tumor-suppressor genes that include *BRAC1*.<sup>74,75</sup> These findings suggest that L1-RTP globally alternates the genome integrity of cells, providing a growth advantage in terms of cancer development. However, due to the low frequency of L1-RTP by environmental carcinogens (approximately one in every 10<sup>5</sup> cells), identification and monitoring of cells positive for L1-RTP during carcinogenesis is problematic. One approach to demonstrate the role of L1-modulated cells in carcinogenesis is to block RTP, for example, by siRNA of L1 mRNA in an organ of interest<sup>76</sup> and evaluate the effects on cancer development.

The carcinogenic effects of HCAs have been attributed to their genotoxic activities.<sup>44,56</sup> However, the PhIP concentration of PhIP in human breast milk has been reported to be approximately 1 pg/ml (3.6 pM),<sup>46</sup> and plasma HCA concentrations were in the nM range.<sup>52</sup> Because PhIP at less than micromolar levels exhibits no genotoxic activity, the level of HCA required to induce genetic alternations remains to be clarified. Here, we demonstrated that nanomolar levels of HCAs induced L1-RTP (Table 1), but micromolar PhIP levels were not genotoxic. Moreover, repeated administration of  $\mu$ M levels of PhIP also induced L1-RTP in the target organ (Figure 8d, Table 1). Taken together with a proposal that low dose of PhIP exerts carcinogenic activity via ER $\alpha$ ,<sup>52,77</sup> data indicate that ER $\alpha$ -dependent L1-RTP is a novel type of genetic

instability that is induced by non-genotoxic effects of environmental compounds. Although humans are exposed to low doses of PhIP, a life-long exposure to low levels of food-borne carcinogens might lead to accumulation of cells positive for genetic alternations caused by L1-RTP.

## MATERIALS AND METHODS

### Cell culture and chemicals

HuH-7 (RCB1366), HepG2 (RCB1886), HEK293T (RCB2202), MCF-7 (RCB1904), Li-7 (RCB1941), Caco-2 (RCB0988) (Riken BioResource Center Cell Bank, Tsukuba, Ibaraki, Japan) and HT1080 (JCRB9113; The Health Science Resources Bank, Tokyo, Japan) were maintained at 37 °C and 5% CO<sub>2</sub> in Dulbecco's modified Eagle's medium supplemented with 10% fetal bovine serum. Aetoxy-forms of HCAs (PhIP: molecular weight 286.3, MeIQx: molecular weight 275.2) were synthesized (NARD Institute, Amagasaki, Hyogo, Japan). Non-acetoxy form PhIP (molecular weight 224.3) was from Toronto Research Chemicals Inc. Other reagents, primary and secondary antibodies used in the current studies are described in Supplementary Information.

### L1-RTP assays

L1-RTP was assayed as described previously,<sup>36,37</sup> using pCEP4/L1mneol/ColE1 (pL1-Neo<sup>R</sup>)<sup>54,55</sup> and pEF06R<sup>33</sup> for colony-formation assay and a PCR-based assay, respectively. For the colony-formation assay, the cells were cultured in the presence of 800  $\mu$ g/ml neomycin, and numbers of neomycin-resistant (Neo<sup>R</sup>) colonies were counted. For the PCR-based assay, DNA was extracted from cells that were treated with the compounds for 2 days (36, 38, Supplementary information). For amplification of *EGFP* cDNA, 5'-ACTGGGTGCTCAGGTAGTGGTT-3' and 5'-GAAGAACGGCATCAAGG TGAA-3' were used as PCR forward and reverse primers, respectively. The forward and reverse PCR primers for detecting human  $\beta$ -actin gene were 5'-TGAACCCCAAGGCCAACCGC-3' and 5'-TTGTGCTGGGTGCCAGGGCA-3', respectively. For mouse  $\beta$ -actin gene, 5'-GAGGGAATCGTGCCTGAC-3' and 5'-AGAAGGAAGGCTGGAAA-3' were used. The conditions of PCR amplification of *EGFP* cDNA and  $\beta$ -actin are described in Supplementary Information of full-methods.

### Transfection of plasmid DNA and siRNAs

In all, 8  $\mu$ g of plasmid DNA was transfected into HuH-7, HepG2, HEK293T, Li-7, Caco-2 and HT1080 using Lipofectamine 2000, whereas it was transfected into MCF-7 cells using Xfect (TAKARA, Otsu, Shiga, Japan). siRNAs were synthesized by Applied Biosystems (Tokyo, Japan). Nucleotide sequence of each siRNA was shown in Supplementary Table S1. As control, Silencer Negative Control siRNA No. 2 (Cat No. AM4637, Life Technologies Corporation, Calsbad, CA, USA) was used. HuH-7 or MCF-7 cells were transfected with 25–100 nM siRNAs using Lipofectamine 2000 (Life Technologies Corporation) or Xfect, respectively. For WB analysis, cell extracts were prepared, as described.<sup>36,37</sup>

### IP assay and immunohistochemical analysis

IP assay was carried out, according to the reported method<sup>36,37</sup> To express ORF1-EGFP, ST-ORF1, flag-tagged C/EBP- $\beta$ , flag-tagged OVA and ST-EGFP, we constructed pORF1-EGFP, pST-ORF1, pFlag-C/EBP- $\beta$ , pFlag-OVA and pST-EGFP. Cells were suspended in IP buffer composed of 20 mM Tris-HCl (pH 7.6), 5 mM EDTA, 150 mM NaCl, 0.5% NP-40 and 10% glycerol. Each 500  $\mu$ g of cell extract was reacted with 4  $\mu$ g of  $\alpha$ AhR or  $\alpha$ EGFP and then recovered with protein G beads (GE Healthcare, Bio-Sciences Corp., Piscataway, NJ, USA). To analyze the association of ORF1 and C/EBP- $\beta$ , antibodies against Flag-tag, EGFP and ORF1 were first reacted, and then immune complexes were recovered with Dynabeads protein G or Dynabeads M-280 streptavidin beads (Life Technologies Corporation). As an input sample, about one-tenth of each extract subjected to IP was loaded onto SDS-PAGE and simultaneously analyzed. The immunohistochemical analysis was done by the reported method.<sup>37</sup>

### HCA-induced chromatin recruitment of ORF1

ORF1 was expressed as a chimeric protein of TAP (tandem affinity purification protein)<sup>64</sup> (EUROSCARF: European Saccharomyces Cerevisiae Archives for Functional Analysis). To express ORF1-TAP and EGFP-TAP, pORF1-TAP and pEGFP-TAP were transfected to HuH-7 cells. The chromatin



fraction was isolated using a Subcellular Protein Fractionation Kit (Thermo Scientific, Waltham, MA, USA), as described.<sup>36</sup> Nuclear insoluble fractions were treated for 30 min with 300 U micrococcal nuclease (Thermo Scientific) at 37 °C and centrifuged for 10 min. After centrifugation at 16 000 g, recovered supernatant was subjected to WB analysis.

### Experiments using hL1-EGFP mice

We used hL1-EGFP transgenic mice of lines No. 4 and No. 67 that had low background of spontaneous L1-RTP during embryogenesis.<sup>37</sup> Each mouse was crossed with heterozygous Ahr-deficient (*Ahr*<sup>+/-</sup>) mice<sup>65</sup> (Riken Bioresource Center). Then, *hL1-EGFP Ahr*<sup>+/-</sup> mice were mated with *Ahr*<sup>+/-</sup> mice to generate homozygous null mutant mice (*hL1-EGFP/Ahr*<sup>-/-</sup>) that carried the hL1-EGFP transgene. Genotyping was performed using DNA extracted from tails. HCAs or the same amount of dimethylsulfoxide (DMSO) were administered intraperitoneally once 2 days. On day 2 after the last injection, mice were killed and the PCR-based assay was done on extracted DNA. To evaluate effects of orally administered PhIP, approximately 3.3 or 1 µg of the compound, which were prepared in 100 µl of saline, were directly injected into the stomach of the mouse six or six times, respectively. Maximum blood concentrations estimated by these doses were of micromolar levels, respectively. As control, the same amount of DMSO was injected. During experiments, no changes in body weight of mice were detected. All animal experiments were approved by the Animal Care and Use Committee of the NCGM Research Institute and conducted in accordance with institutional procedures.

### Protocol of administration of fulvestrant into hL1-EGFP mice

Effects of 7.7 mg/kg of fulvestrant on the induction of L1-RTP by PhIP were evaluated. Fulvestrant was intraperitoneally injected 4 h before administration of PhIP. The similar regimens of administration were repeated three times once 2 days. On day 2 after the last injection, genomic DNA extracted from each organ was subjected to the PCR-based assay.

### Statistics

Statistical significance was evaluated using Mann–Whitney *U* test. Numbers of test samples were more than four. Values of <0.05 were considered to be statistically significant.

### CONFLICT OF INTEREST

The authors declare no conflict of interest.

### ACKNOWLEDGEMENTS

We are grateful to Drs Elena. T Luning Prak (University of Pennsylvania Medical Center), Gilbert Nicolas (University of Michigan Medical School) and Gabriele Vielhaber (Symrise, Germany) for providing pEF06R, pCEP4/L1mneo/ColE1 and MNF, respectively. An antibody to AhRR was a kind gift from Dr Mark E Hahn (Woods Hole Oceanographic Institution). This work was supported in parts by a Grant-in-Aid for Research from the Ministry of Health, Labor and Welfare of Japan (09156296), and a research grant for the Log-range Research Initiative (LRI) from Japan Chemical Industry Association (JCIA). NO was an applicant supported by Grant-in-Aid from the Tokyo Biochemical Research Foundation. This work was supported in part by a Joint-Use Research facility, Hyogo College of Medicine.

### REFERENCES

- 1 Bannert N, Kurth R. Retroelements and the human genome: new perspectives on an old relation. *Proc Natl Acad Sci USA* 2004; **101**: 14572–14579.
- 2 Brouha B, Schustak J, Badge RM, Lutz-Prigge S, Farley AH, Moran JV *et al*. Hot L1s account for the bulk of retrotransposition in the human population. *Proc Natl Acad Sci USA* 2003; **100**: 5280–5285.
- 3 Goodier JL, Kazazian HH Jr. Retrotransposons revisited: the restraint and rehabilitation of parasites. *Cell* 2008; **135**: 23–35.
- 4 Babushok DV, Kazazian HH Jr. Progress in understanding the biology of the human mutagen LINE-1. *Hum Mutat* 2007; **28**: 527–539.
- 5 Hohjoh H, Singer MF. Cytoplasmic ribonucleoprotein complexes containing human LINE-1 protein and RNA. *EMBO J* 1996; **15**: 630–639.
- 6 Goodier JL, Zhang L, Vetter MR, Kazazian HH Jr. LINE-1 ORF1 protein localizes in stress granules with other RNA-binding proteins, including components of RNA interference RNA-induced silencing complex. *Mol Cell Biol* 2007; **27**: 6469–6483.

- 7 Wei W, Gilbert N, Ooi SL, Lawler JF, Ostertag EM, Kazazian HH Jr *et al*. Human L1 retrotransposition: *cis* preference versus trans complementation. *Mol Cell Biol* 2001; **21**: 1429–1439.
- 8 Martin SL, Cruceanu M, Branciforte D, Wai-Lun Li P, Kwok SC, Hodges RS *et al*. LINE-1 retrotransposition requires the nucleic acid chaperone activity of the ORF1 protein. *J Mol Biol* 2005; **348**: 549–561.
- 9 Mathias SL, Scott AF, Kazazian HH Jr, Boeke JD, Gabriel A. Reverse transcriptase encoded by a human transposable element. *Science* 1991; **254**: 1808–1810.
- 10 Feng Q, Moran JV, Kazazian HH Jr, Boeke JD. Human L1 retrotransposon encodes a conserved endonuclease required for retrotransposition. *Cell* 1996; **87**: 905–916.
- 11 Jurka J. Sequence patterns indicate an enzymatic involvement in integration of mammalian retrotransposons. *Proc Natl Acad Sci USA* 1997; **94**: 1872–1877.
- 12 Gilbert N, Luts S, Morrish TA, Moran JV. Multiple fates of L1 retrotransposition intermediates in cultured human cells. *Mol Cell Biol* 2005; **25**: 7780–7795.
- 13 Gasior SL, Wakeman TP, Xu B, Deininger PL. The human LINE-1 retrotransposon creates DNA double-strand breaks. *J Mol Biol* 2006; **357**: 1383–1393.
- 14 Dewannieux M, Esnault C, Heidmann T. LINE-mediated retrotransposition of marked Alu sequences. *Nat Genet* 2003; **35**: 41–48.
- 15 Wallace N, Wagstaff BJ, Deininger PL, Roy-Engel AM. LINE-1 ORF1 protein enhances Alu SINE retrotransposition. *Gene* 2008; **419**: 1–6.
- 16 Raiz J, Damert A, Chira S, Held U, Klawitter S, Hamdorf M *et al*. The non-autonomous retrotransposon SVA is trans-mobilized by the human LINE-1 protein machinery. *Nucleic Acids Res* 2012; **40**: 1666–1683.
- 17 Vitullo P, Sciamanna I, Baiocchi M, Sinibaldi-Vallebona P, Spadafora C. LINE-1 retrotransposon copies are amplified during murine early embryo development. *Mol Reprod Dev* 2012; **79**: 118–127.
- 18 Beraldi R, Pittoggi C, Sciamanna I, Mattei E, Spadafora C. Expression of LINE-1 retrotransposons is essential for murine preimplantation development. *Mol Reprod Dev* 2006; **73**: 279–287.
- 19 Belancio VP, Hedges DJ, Deininger P. Mammalian non-LTR retrotransposons: for better or worse, in sickness and in health. *Genome Res* 2008; **18**: 343–358.
- 20 Hancks DC, Kazazian HH Jr. Active human retrotransposons: variation and disease. *Curr Opin Genet Dev* 2012; **22**: 191–203.
- 21 Georgiou I, Noutsopoulos D, Dimitriadou E, Markopoulos G, Apergi A, Lazaros L *et al*. Retrotransposon RNA expression and evidence for retrotransposition events in human oocytes. *Hum Mol Genet* 2009; **18**: 1221–1228.
- 22 Kano H, Godoy I, Courtney C, Vetter MR, Gerton GL, Ostertag EM *et al*. L1 retrotransposition occurs mainly in embryogenesis and creates somatic mosaicism. *Genes Dev* 2009; **23**: 1303–1312.
- 23 Macia A, Muñoz-Lopez M, Cortes JL, Hastings RK, Morell S, Lucena-Aguilar G *et al*. Epigenetic control of retrotransposon expression in human embryonic stem cells. *Mol Cell Biol* 2011; **31**: 300–316.
- 24 Coufal NG, Garcia-Perez JL, Peng GE, Yeo GW, Mu Y, Lovci MT *et al*. L1 retrotransposition in human neural progenitor cells. *Nature* 2009; **460**: 1127–1131.
- 25 Baillie JK, Barnett MW, Upton KR, Gerhardt DJ, Richmond TA, De Sapio F *et al*. Somatic retrotransposition alters the genetic landscape of the human brain. *Nature* 2011; **479**: 534–537.
- 26 Coufal NG, Garcia-Perez JL, Peng GE, Marchetto MC, Muotri AR, Mu Y *et al*. Ataxia telangiectasia mutated (ATM) modulates long interspersed element-1 (L1) retrotransposition in human neural stem cells. *Proc Natl Acad Sci USA* 2011; **108**: 20382–20387.
- 27 Morse B, Rotherg PG, South VJ, Spandorfer JM, Astrin SM. Insertional mutagenesis of the *myc* locus by a LINE-1 sequence in a human breast carcinoma. *Nature* 1988; **333**: 87–90.
- 28 Miki Y, Nishisho I, Horii A, Miyoshi Y, Utsunomiya J, Kinzler KW *et al*. Disruption of the APC gene by a retrotranspositional insertion of L1 sequence in a colon cancer. *Cancer Res* 1992; **52**: 643–645.
- 29 Iskow RC, McCabe MT, Mills RE, Torene S, Pittard WS, Neuwald AF *et al*. Natural mutagenesis of human genomes by endogenous retrotransposons. *Cell* 2010; **141**: 1253–1261.
- 30 Ting DT, Lipson D, Paul S, Brannigan BW, Akhavanfard S, Coffman EJ *et al*. Aberrant overexpression of satellite repeats in pancreatic and other epithelial cancers. *Science* 2011; **331**: 593–596.
- 31 Kazazian HH Jr. Mobile DNA transposition in somatic cells. *BMC Biol* 2011; **29**: 62.
- 32 Lee E, Iskow R, Yang L, Gokcumen O, Haseley P, Luquette LJ 3rd *et al*. Landscape of Somatic Retrotransposition in Human Cancers. *Science* 2012; **337**: 967–971.
- 33 Farkash EA, Kao GD, Horman SR, Prak ET. Gamma radiation increases endonuclease-dependent L1 retrotransposition in a cultured cell assay. *Nucleic Acids Res* 2006; **34**: 1196–1204.
- 34 Kale SP, Moore L, Deininger PL, Roy-Engel AM. Heavy metals stimulate human LINE-1 retrotransposition. *Int J Environ Res Public Health* 2005; **2**: 14–23.
- 35 Stribinskis V, Ramos KS. Activation of human long interspersed nuclear element 1 retrotransposition by benzo(a)pyrene, an ubiquitous environmental carcinogen. *Cancer Res* 2006; **66**: 2616–2620.

- 36 Okudaira N, Iijima K, Koyama T, Minemoto Y, Kano S, Mimori A *et al*. Induction of long interspersed nucleotide element-1 (L1) retrotransposition by 6-formylindolo[3,2-b]carbazole (FICZ), a tryptophan photoproduct. *Proc Natl Acad Sci USA* 2010; **107**: 18487–18492.
- 37 Okudaira N, Goto M, Yanobu-Takanashi R, Tamura M, An A, Abe Y *et al*. Involvement of retrotransposition of long interspersed nucleotide element-1 in skin tumorigenesis induced by 7,12-dimethylbenz[a]anthracene and 12-O-tetradecanoylphorbol-13-acetate. *Cancer Sci* 2011; **102**: 2000–2006.
- 38 Hoffman EC, Reyes H, Chu FF, Sander F, Conley LH, Brooks BA *et al*. Cloning of a factor required for activity of the Ah (dioxin) receptor. *Science* 1991; **252**: 954–958.
- 39 Hahn ME. Aryl hydrocarbon receptors: diversity and evolution. *Chem Biol Interact* 2002; **141**: 131–160.
- 40 Beischlag TV, Luis Morales J, Hollingshead BD, Perdew GH. The aryl hydrocarbon receptor complex and the control of gene expression. *Crit Rev Eukaryot Gene Expr* 2008; **18**: 207–250.
- 41 McIntosh BE, Hogenesch JB, Bradfield CA. Mammalian Per-Arnt-Sim proteins in environmental adaptation. *Annu Rev Physiol* 2010; **72**: 625–645.
- 42 Eguchi H, Ikuta T, Tachibana T, Yoneda Y, Kawajiri K. A nuclear localization signal of human aryl hydrocarbon receptor nuclear translocator/hypoxia-inducible factor 1beta is a novel bipartite type recognized by the two components of nuclear pore-targeting complex. *J Biol Chem* 1997; **272**: 17640–17647.
- 43 Wiseman M. The second World Cancer Research Fund/American Institute for Cancer Research expert report. Food, nutrition, physical activity, and the prevention of cancer: a global perspective. *Proc Nutr Soc* 2008; **67**: 253–256.
- 44 Sugimura T, Wakabayashi K, Nakagama H, Nagao M. Heterocyclic amines: mutagens/carcinogens produced during cooking of meat and fish. *Cancer Sci* 2004; **95**: 290–299.
- 45 Layton DW, Bogen KT, Knize MG, Hatch FT, Johnson VM, Felton JS. Cancer risk of heterocyclic amines in cooked foods: an analysis and implications for research. *Carcinogenesis* 1995; **16**: 39–52.
- 46 Scott KA, Turesky RJ, Wainman BC, Josephy PD. Hplc/electrospray ionization mass spectrometric analysis of the heterocyclic aromatic amine carcinogen 2-amino-1-methyl-6-phenylimidazo[4,5-b]pyridine in human milk. *Chem Res Toxicol* 2007; **20**: 88–94.
- 47 Ito N, Hasegawa R, Sano M, Tamano S, Esumi H, Takayama S *et al*. A new colon and mammary carcinogen in cooked food, 2-amino-1-methyl-6-phenylimidazo[4,5-b]pyridine (PhIP). *Carcinogenesis* 1991; **12**: 1503–1506.
- 48 Shirai T, Sano M, Tamano S, Takahashi S, Hirose M, Futakuchi M *et al*. The prostate: a target for carcinogenicity of 2-amino-1-methyl-6-phenylimidazo[4,5-b]pyridine (PhIP) derived from cooked foods. *Cancer Res* 1997; **57**: 195–198.
- 49 Nakai Y, Nelson WG, De Marzo AM. The dietary charred meat carcinogen 2-amino-1-methyl-6-phenylimidazo[4,5-b]pyridine acts as both a tumor initiator and promoter in the rat ventral prostate. *Cancer Res* 2007; **67**: 1378–1384.
- 50 Nishikawa A, Imazawa T, Kuroiwa Y, Kitamura Y, Kanki K, Ishii Y *et al*. Induction of colon tumors in C57BL/6J mice fed MeIQx, IQ, or PhIP followed by dextran sulfate sodium treatment. *Toxicol sci* 2005; **84**: 243–248.
- 51 Ohgaki H, Hasegawa H, Suenaga M, Sato S, Takayama S, Sugimura T. Carcinogenicity in mice of a mutagenic compound, 2-amino-3,8-dimethylimidazo[4,5-f]quinoxaline (MeIQx) from cooked foods. *Carcinogenesis* 1987; **8**: 665–668.
- 52 Lauber SN, Ali S, Gooderham NJ. The cooked food derived carcinogen 2-amino-1-methyl-6-phenylimidazo[4,5-b]pyridine is a potent oestrogen: a mechanistic basis for its tissue-specific carcinogenicity. *Carcinogenesis* 2004; **25**: 2509–2517.
- 53 Ema M, Morita M, Ikawa S, Tanaka M, Matsuda Y, Gotoh O *et al*. Two new members of the murine Sim gene family are transcriptional repressors and show different expression patterns during mouse embryogenesis. *Mol Cell Biol* 1996; **16**: 5865–5875.
- 54 Gilbert N, Lutz-Prigge S, Moran JV. Genomic deletions created upon LINE-1 retrotransposition. *Cell* 2002; **110**: 315–325.
- 55 Wei W, Morrish TA, Alich RS, Moran JV. A transient assay reveals that cultured human cells can accommodate multiple LINE-1 retrotransposition events. *Anal Biochem* 2000; **284**: 435–438.
- 56 Schut HA, Snyderwine EG. DNA adducts of heterocyclic amine food mutagens: implications for mutagenesis and carcinogenesis. *Carcinogenesis* 1999; **20**: 353–368.
- 57 Kleman MI, Overvik E, Mason GG, Gustafsson JA. In vitro activation of the dioxin receptor to a DNA-binding form by food-borne heterocyclic amines. *Carcinogenesis* 1992; **13**: 1619–1624.
- 58 Fritsche E, Schäfer C, Calles C, Bernsmann T, Bernshausen T, Wurm M *et al*. Lightening up the UV response by identification of the arylhydrocarbon receptor as a cytoplasmic target for ultraviolet B radiation. *Proc Natl Acad Sci USA* 2007; **104**: 8851–8856.
- 59 Wincent E, Bengtsson J, Mohammadi Bardbori A, Alsberg T, Luecke S, Rannug U *et al*. Inhibition of cytochrome P4501-dependent clearance of the endogenous agonist FICZ as a mechanism for activation of the aryl hydrocarbon receptor. *Proc Natl Acad Sci USA* 2012; **109**: 4479–4484.
- 60 Karchner SI, Jenny MJ, Tarrant AM, Evans BR, Kang HJ, Bae I *et al*. The active form of human aryl hydrocarbon receptor (AHR) repressor lacks exon 8, and its Pro 185 and Ala 185 variants repress both AHR and hypoxia-inducible factor. *Mol Cell Biol* 2009; **29**: 3465–3477.
- 61 Osborne CK, Wakeling A, Nicholson RI. Fulvestrant: an oestrogen receptor antagonist with a novel mechanism of action. *Br J Cancer* 2004; **90**: S2–S6.
- 62 Weiss C, Faust D, Dürk H, Kolluri SK, Pelzer A, Schneider S *et al*. TCDD induces c-jun expression via a novel Ah (dioxin) receptor-mediated p38-MAPK-dependent pathway. *Oncogene* 2005; **24**: 4975–4983.
- 63 Ishizaka Y, Okudaira N, Okamura T. Regulation of retrotransposition of long interspersed element-1 by mitogen-activated protein kinases. In: Da Silva Xavier G (ed). *Protein Kinases/Book 1*. InTecOpen: Croatia, pp 187–198 (<http://www.intechopen.com/books/protein-kinases>).
- 64 Puig O, Caspary F, Rigaut G, Rutz B, Bouveret E, Bragado-Nilsson E *et al*. The tandem affinity purification (TAP) method: a general procedure of protein complex purification. *Methods* 2001; **24**: 218–229.
- 65 Mimura J, Yamashita K, Nakamura K, Morita M, Takagi TN, Nakao K *et al*. Loss of teratogenic response to 2,3,7,8-tetrachlorodibenzo-p-dioxin (TCDD) in mice lacking the Ah (dioxin) receptor. *Genes Cells* 1997; **2**: 645–654.
- 66 Hahn ME, Allan LL, Sherr DH. Regulation of constitutive and inducible AHR signaling: complex interactions involving the AHR repressor. *Biochem Pharmacol* 2009; **77**: 485–497.
- 67 Woodcock DM, Lawler CB, Linsenmeyer ME, Doherty JP, Warren WD. Asymmetric methylation in the hypermethylated CpG promoter region of the human L1 retrotransposon. *J Biol Chem* 1997; **272**: 7810–7816.
- 68 Muotri AR, Marchetto MC, Coufal NG, Oefner R, Yeo G, Nakashima K *et al*. L1 retrotransposition in neurons is modulated by MeCP2. *Nature* 2010; **468**: 443–446.
- 69 Herman JG, Graff JR, Myöhänen S, Nelkin BD, Baylin SB. Methylation-specific PCR: a novel PCR assay for methylation status of CpG islands. *Proc Natl Acad Sci USA* 1996; **93**: 9821–9826.
- 70 Quintana FJ, Basso AS, Iglesias AH, Korn T, Farez MF, Bettelli E *et al*. Control of T(reg) and T(H)17 cell differentiation by the aryl hydrocarbon receptor. *Nature* 2008; **453**: 65–71.
- 71 Veldhoen M, Hirota K, Westendorf AM, Buer J, Dumoutier L, Renaud JC *et al*. The aryl hydrocarbon receptor links TH17-cell-mediated autoimmunity to environmental toxins. *Nature* 2008; **453**: 106–109.
- 72 Shimizu Y, Nakatsuru Y, Ichinose M, Takahashi Y, Kume H, Mimura J *et al*. Benzo[a]pyrene carcinogenicity is lost in mice lacking the aryl hydrocarbon receptor. *Proc Natl Acad Sci USA* 2000; **97**: 779–782.
- 73 Symer DE, Connelly C, Szak ST, Caputo EM, Cost GJ, Parmigiani G *et al*. Human L1 retrotransposition is associated with genetic instability in vivo. *Cell* 2002; **110**: 327–338.
- 74 Belancio VP, Roy-Engel AM, Deininger PL. All y'all need to know 'bout retroelements in cancer. *Semin Cancer Biol* 2010; **20**: 200–210.
- 75 Konkel MK, Batzer MA. A mobile threat to genome stability: the impact of non-LTR retrotransposons upon the human genome. *Semin Cancer Biol* 2010; **20**: 211–221.
- 76 Oricchio E, Sciamanna I, Beraldi R, Tolstonog GV, Schumann GG, Spadafora C. Distinct roles for LINE-1 and HERV-K retroelements in cell proliferation, differentiation and tumor progression. *Oncogene* 2007; **26**: 4226–4233.
- 77 Lauber SN, Gooderham NJ. The cooked meat derived genotoxic carcinogen 2-amino-3-methylimidazo[4,5-b]pyridine has potent hormone-like activity: mechanistic support for a role in breast cancer. *Cancer Res* 2007; **67**: 9597–9602.



This work is licensed under the Creative Commons Attribution-NonCommercial-No Derivative Works 3.0 Unported License. To view a copy of this license, visit <http://creativecommons.org/licenses/by-nc-nd/3.0/>

Supplementary Information accompanies the paper on the Oncogene website (<http://www.nature.com/onc>)